This article has been accepted for publication in IEEE Transactions on Applied Superconductivity. This is the author's version which has not been fully edited and content may change prior to final publication. Citation information: DOI 10.1109/TASC.2023.3238991

Chemical Solution Deposition of MTiO$_3$ (M = Ca, Sr, and Ba) based Buffer Layer prior to Coated Conductors architectures

Hannes Rijckaert, Klaartje De Buysser, and Isabel Van Driessche

***Abstract*—Chemical solution deposition (CSD) approach was introduced in this work to simplify and to optimize the trifluoracetic based MTiO$_3$ (MTO, M = Ca, Sr, and Ba) precursor solution, leading to the high shelf-life and the purity. Growing these MTO solutions on (100) LaAlO$_3$ single-crystal substrates yields (h00) oriented and dense MTO buffer layers. Whereas it is clear that the roughness of MTO films and the lattice mismatch between MTO buffer layer and superconducting YBa$_2$Cu$_3$O$_{7-\delta}$ film is crucial for the film formation.**

***Index Terms* — buffer layer, chemical solution deposition, coated conductor, thin film, titanate.**

I. INTRODUCTION

The coated conductor architecture was developed to exploit the potential of low-cost high temperature superconductors with excellent performance[1, 2]. Prior to low-cost industrial production, the coated conductor architecture which consist of superconducting REBa$_2$Cu$_3$O$_{7-\delta}$ (REBCO, RE = Rare Earth or yttrium) compound as a thin film on cube-textured Ni based alloy tapes was developed by Chemical Solution Deposition (CSD) methods [3, 4]. Before the epitaxial growth of REBCO film, a stack of buffer layers is applied on the metallic substrate as a diffusion barrier which is also required to transfer the strong texture of the underlying substrate. State-of-the-art coated conductor structures are mainly based on fluorite-like CeO$_2$ based buffer stacks that consist of a sequence of several different buffer layers [5]. Nevertheless, this architecture still suffers from the reactivity of CeO$_2$ with REBCO material, leading to the undesired BaCeO$_3$ phase and inferior film texture.

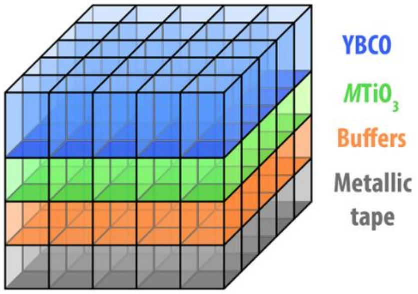

Fig. 1. Schematic overview of solution-derived superconducting YBCO and MTO buffer films on buffered metallic tape.

Titanate-based materials (MTiO$_3$, MTO) like SrTiO$_3$ (STO, 3.91 Å) or CaTiO$_3$ (CTO, 3.82 Å) have a minimal lattice mismatch with REBCO material and Ni based alloy tape, exhibit a small oxygen diffusion coefficient and offer good chemical stability towards both the metallic substrate and the REBCO. However, the interdiffusion of Sr^{2+} and Ti^{4+} in REBCO can occur if STO material is treated at high temperature annealing [6].Thus, these materials are promising as it can act as a single buffer layer and form a template bridge between the superconducting YBCO layer and the metallic substrate. In literature, several authors [7-10] have succeeded to grow (h00)-oriented titanate-based materials on one single-crystal substrate like LaAlO$_3$ via CSD technique with a suitable Metal-Organic Decomposition (MOD) method. Generally in MOD method, organometallic salts are dissolved in a proper organic solvent to produce low-cost epitaxial thin films without the requirement of a high-vacuum system [11, 12]. Siegal *et al.*[13] and Kunert *et al.*[14] have demonstrated the opportunity to use CSD method to grow (h00)-oriented STO films on Ni-based tapes via the introduction of the thick barium-substituted CTO as a seed layer. Nevertheless, the major drawback of these works is the difficulty in synthesizing and handling the precursors based on humidity sensitive alkoxides. The texture quality of titanate-based buffer layers depends on water-free and stable MTO precursor solutions and its thermal processing [15].

In this work, the CSD route of fluorine based titanate buffer layers is introduced as trifluoroacetate (TFA) route. These TFA-based MTO solutions were simplified and optimized in this work, resulting in the stable MTO solution with a high purity. This reliable method led to significant advances toward more viable MTO layer processing. After the deposition onto single crystal LaAlO$_3$ (100) substrates, it yields to (h00)-oriented MTO layers after the suitable crystallization step. Subsequently, solution-derived YBCO film was grown on these MTO layers to check the final morphological properties of the superconducting film. This method and acknowledge will simplify

Manuscript receipt and acceptance dates will be inserted here. Hannes Rijckaert acknowledges support and funding as postdoctoral fellow fundamental research of the Research Foundation-Flanders (FWO, Grant number 1273621N). *(Corresponding author: Hannes Rijckaert)*

H. Rijckaert, K. De Buysser and I. Van Driessche are with the Department of Chemistry, Ghent University, SCRiPTS, 9000 Ghent, Belgium (e-mail: hannes.rijckaert@ugent.be).

Color versions of one or more of the figures in this paper are available online at http://ieeexplore.ieee.org.

Digital Object Identifier will be inserted here upon acceptance.

Template version 8.0d, 22 August 2017. IEEE will put copyright information in this area
See http://www.ieee.org/publications_standards/publications/rights/index.html for more information.

© 2023 IEEE. Personal use is permitted, but republication/redistribution requires IEEE permission. See https://www.ieee.org/publications/rights/index.html for more information.
Authorized licensed use limited to: University of Gent. Downloaded on January 24,2023 at 08:34:40 UTC from IEEE Xplore. Restrictions apply.

the cumbersome transfer of *M*TO buffer film from one-single crystal substrate to flexible buffered metallic tape (Figure 1).

II. Experimental Details

A. Preparation of the MTO and YBCO precursor solutions.

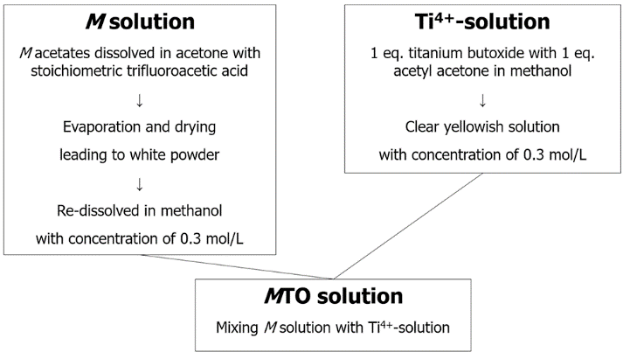

Fig. 2 Summary of the preparation route for *M*TO solutions.

The preparation routes for the *M*TO precursors used in this work are shown in figure 2. The *M*TO solutions were prepared by first dissolved the *M* acetates (purity > 99.99%, Alfa Aesar) in 3 mL acetone with stoichiometric trifluoroacetic acid (TFAH, 99.5+%, Alfa Aesar). The addition of TFAH led to transform the *M* acetates into *M* trifluoroacetates. The obtained TFA-based solutions were evaporated under vacuum using a rotary evaporator, resulting in a highly viscous residue. This residue was dried in a drying furnace at 60 °C for 6 hours. The dried white powder is re-dissolved in methanol (99.5%, Carl Roth), yielding to a yellowish and clear *M* solution with a final concentration of 0.3 mol/L. Second, Ti^{4+}-solution was prepared by adding 1 eq. Titanium Butoxide (TiB, Sigma Aldrich, ≥ 97%) to 1 eq. acetyl acetone (HAcac, Acros Organics, ≥ 99%) in methanol to obtain a final Ti^{4+}-concentration of 0.3 mol/L. Final, *M* solution is mixed with Ti^{4+} solution, leading to *M*TO solution. The low-fluorine YBCO solutions used in this work were prepared following the protocol reported in ref. [16]. In summary, The YBCO solution was prepared by dissolving $Y(C_3H_5O_2)_3$, $Ba(CF_3CO_2)_2$, and $Cu(C_3H_5O_2)_2$ in methanol with a Y:Ba:Cu stoichiometric ratio of 1:2:3.

B. Growth of MTO and YBCO films on single crystal substrates

The *M*TO solutions were coated on polished (100)-$LaAlO_3$ one-single crystal substrate (Crystek GmbH) by means of spin-coating (50 rps for 30 s). Prior to deposition, the $LaAlO_3$ substrates were chemically and thermally treated in order to remove impurities and to reconstruct the surface termination as described in the literature [17, 18]. The as-deposited films were first pyrolyzed at 200 °C for 5 min on a hot plate in the ambient to burn out the organic components. Subsequently, the pyrolyzed films were heated with a heating rate of 9 °C/min to 900 °C for 120 min in a flowing humid Ar/5% H_2 atmosphere. The inlet gas with a flow rate of 600 mL/min was humidified by passing it through a water bath maintained at 23 °C, leading to an oxygen partial pressure of 10^{-14} atm. This atmosphere was chosen in order to preserve compatibility of the processing conditions with commonly used metallic substrates in the coated conductor architectures. The *M*TO buffered $LaAlO_3$ was untreated before the deposition via spin-coating. As-deposited films underwent a thermal treatment (pyrolysis, crystallization and annealing) according to the protocol reported in ref. [16].

C. Characterization

To understand the thermal decomposition of the *M*TO precursor solution, thermogravimetrical analysis (TGA) were performed on dried *M*TO powders with a Netzsch Model STA 449F3 Jupiter system with the heating rate of 10°C/min and an air flow rate of 120 mL/min. The crystallographic properties and phase purity were investigated by X-Ray Diffraction (XRD, Bruker D8, Cu Kα, Bragg-Brentano geometry). An offset coupled θ/2θ measurement method was used to eliminate one-single crystal diffraction coming from the substrate. The surface morphology and the film microstructure in the cross-section of YBCO and *M*TO buffer films was analyzed by a FEI Nova Nanolab Dual Beam Focused Ion Beam (FIB) Scanning Electron Microscopy (SEM).

III. Results and Discussion

A. MTO precursor solution characterization.

In this work, a *M*TO precursor is prepared starting from *M* acetates mixed with stoichiometric TFA in acetone, where it yields in *M* trifluoroacetates. Compared to the conventional method as described in literature[12, 19, 20], we used acetone as the solvent instead of H_2O. The use of H_2O as solvent exhibits an uncontrolled amount of water (>3 wt%) and other chemical impurities (a.o. acetic acid) [20]. To avoid this, in our previous work [11] we have introduced acetone as solvent, leading to highly purity *M* trifluoroacetates without any undesired chemical impurities. Another advantage is that using stoichiometric TFA is beneficial to the environment and can also reduce the corrosion of equipment during the evaporation step.

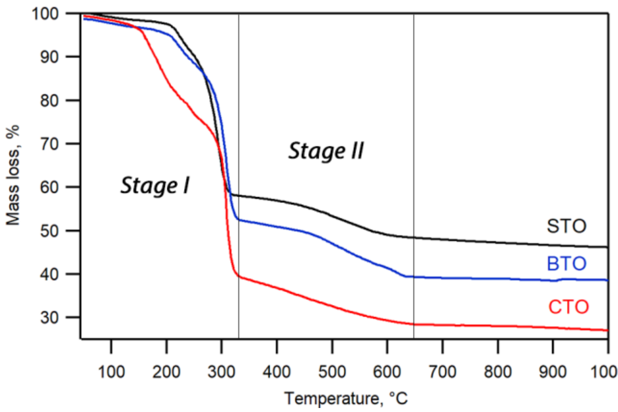

Fig. 3. TGA record of dried *M*TO precursor solution with heating ramp of 10 °C/min and air atmosphere.

© 2023 IEEE. Personal use is permitted, but republication/redistribution requires IEEE permission. See https://www.ieee.org/publications/rights/index.html for more information.
Authorized licensed use limited to: University of Gent. Downloaded on January 24,2023 at 08:34:40 UTC from IEEE Xplore. Restrictions apply.

This article has been accepted for publication in IEEE Transactions on Applied Superconductivity. This is the author's version which has not been fully edited and content may change prior to final publication. Citation information: DOI 10.1109/TASC.2023.3238991

These dried *M* trifluoroacetates can be easily dissolved in methanol or 1-butanol, making these precursors attractive for CSD method. Next, titanium butoxide was introduced as Ti^{4+} precursor however it is extremely sensitive to water (absorbed H_2O from humidity), which can lead to forming of precipitation. Acetylacetone has often been used in CSD process as a chemical additive to reduce the reactivity of metallic alkoxides [21]. Therefore, 1 equivalent acetyl acetone is added to 1 equivalent titanium butoxide in methanol, leading To modified $TiO(acac)_2$ complex precursor in methanol [22]. This modified $TiO(acac)_2$ precursor is added to *M* trifluoroacetate dissolved in methanol, leading to a *M*TO ink with high shell life for long time, confirming that the hydrolysis-condensation of Ti^{4+} precursor is avoided.

As the decomposition of the metal organic precursor is one of the critical steps in CSD method to grow a high-quality metal oxide thin films [23], TGA analysis can give detailed understanding of the temperature dependency of the decomposition. Figure 3 shows the TGA record of dried *M*TO inks and it can be seen that the weight loss starts at 100°C and the precursor is fully decomposed at 650 °C with a total mass loss of 70% for CTO, 60% for BTO, and 50% for STO. The mass loss as a function of temperature can clearly be divided in two separate stages. Between 100 °C and 325 °C (Stage I in Figure 3), all of the samples show huge mass loss and is due to the degradation of M trifluoroacetate as early works affirmed that *M* trifluoroacetate salts start to decompose at the range between 200 °C-250 °C [11, 19]. Above 325 °C, TGA signals also show small mass loss and is probably related to the decomposition of acetyl acetone as it has shown that coordinated ligands are more thermally stable [24]. Between 325 °C and 640 °C (Stage II in Figure 3) is related to the formation of the intermediate phases such as metal oxyfluoride and titanium oxide that will react with each to form cubic *M*TO phase above 640 °C.

B. Growth and characterization of MTO film on single crystal substrate.

The formation of metal oxyfluoride as an intermediate phase is beneficial over the formation of $BaCO_3$, as the latter can disrupt the *M*TO formation due to its high decomposition temperature [12]. On the other hand, metal fluoride is stable up to high temperatures, but can be decomposed around 640 °C by the addition of a humid atmosphere during the crystallization step of *M*TO film. Pollefeyt *et al.* [7] has confirmed that the humid thermal treatment gave rise to strongly textured, dense, and terraced STO films. Therefore, in this work a humid forming gas is introduced to grow *M*TO film on one-single crystal $LaAlO_3$ substrate. After the deposition and thermal treatment of *M*TO films at 900 °C, the quality of the *M*TO thin film was analyzed by θ-2θ diffraction patterns. The XRD patterns (Figure 4) show that (*h*00) oriented films are formed due to the presence of (200) *M*TO peak (CTO 2θ = 47.6°, BTO 2θ = 45.5°, and STO 2θ = 46.6°). Based on XRD peaks, we can observed that BTO film show lower crystallinity compared to STO and CTO films as BTO (110) and (111) reflections are present.

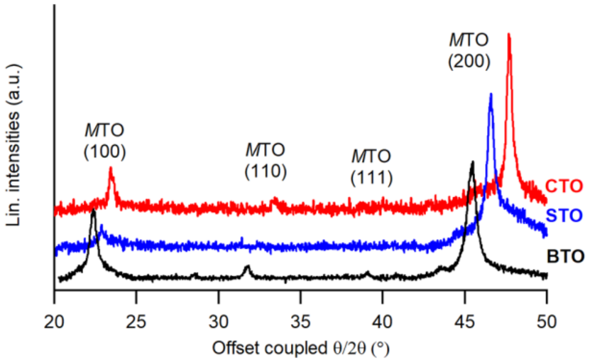

Fig. 4. Offset XRD patterns of CTO, STO, and BTO films after wet thermal processing. Peak at 2θ = 44.9° is a reflection by the secondary radiation of x-ray tube.

It is also observed on SEM images (Figure 5) that *M*TO films show different morphology but CTO and STO films exhibit a good a-axis orientation of the films and the rectangular shape of the terraces while BTO film show less a-axis orientation. This terracing is due to the facilitated decomposition of metal precursor and removal of residual carbon, leading to an improved film growth and better texturing. The cross-sectional SEM images (Figure 5) exhibit very rough BTO film with the thickness between 35 and 170 nm while STO film show a less roughness with the thickness between 110 and 140 nm. CTO film show smooth film with the thickness of 115±5 nm. All of these *M*TO films show a dense film with no or few secondary phases and no porosity. The microstructure of STO and CTO films in this work is similar to the ones reported by Kunert *et al.* [14] and Clem *et al.* [25], showing the high potential of these fluorine based *M*TO precursors.

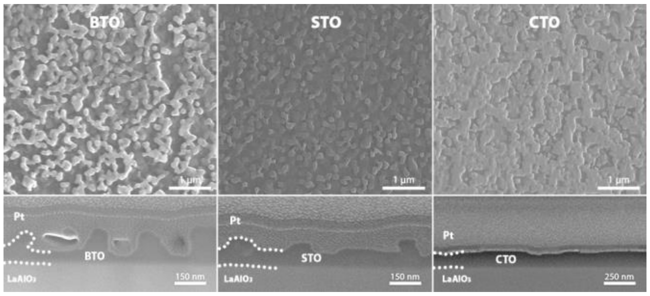

Fig. 5. SEM images showing the surface morphology (top) and cross-sectional view (bottom) of BTO, STO, and CTO thin films on $LaAlO_3$ substrate after wet thermal processing. Pt is a protective layer, deposited via FIB-SEM.

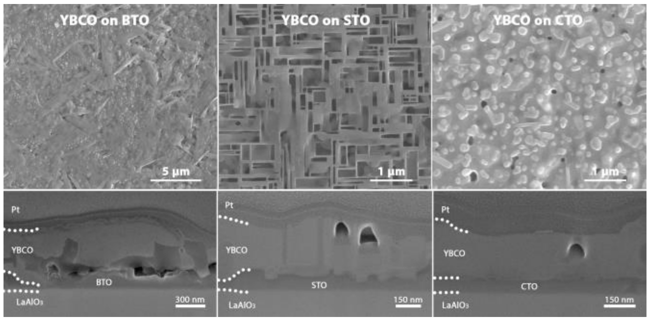

Fig. 6. SEM images showing the surface morphology (top) and cross-sectional view (bottom) of YBCO film, grown on *M*TO buffered $LaAlO_3$ substrate. Pt is a protective layer, deposited via FIB-SEM.

© 2023 IEEE. Personal use is permitted, but republication/redistribution requires IEEE permission. See https://www.ieee.org/publications/rights/index.html for more information.
Authorized licensed use limited to: University of Gent. Downloaded on January 24,2023 at 08:34:40 UTC from IEEE Xplore. Restrictions apply.

This article has been accepted for publication in IEEE Transactions on Applied Superconductivity. This is the author's version which has not been fully edited and content may change prior to final publication. Citation information: DOI 10.1109/TASC.2023.3238991

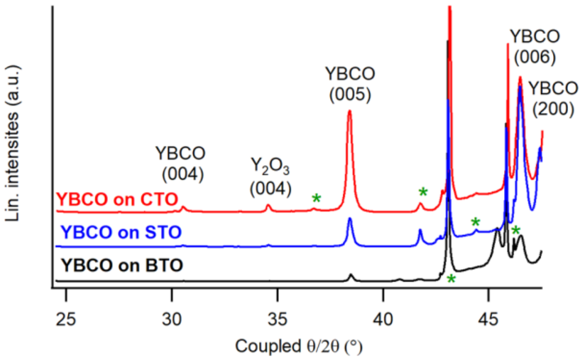

Fig. 7. XRD patterns of YBCO film, grown on *M*TO buffered $LaAlO_3$ substrate. ($LaAlO_3$ and YBCO reflection by the secondary radiation of x-ray tube is marked with green asterisk.)

TABLE I: COMPARISON OF THE CALCULATED LATTICE PARAMETERS AND LATTICE MISMATCHES BETWEEN THE *M*TO AND $YBCO_6$ MATERIAL.

Material	Calculated lattice parameter *a*	Mismatch with $YBCO_6$ (3.86 Å)[a]
CTO	3.82 Å	1.05%
STO	3.90 Å	1.03%
BTO	3.98 Å	3.02%

[a] Tetragonal $YBCO_6$ crystal will change to orthorhombic $YBCO_{7-x}$ crystal with the introduction of oxygen in the lattice during the oxygenation step. However, $YBCO_{7-x}$ unit cell parameters change continuously when the oxygenation changes.

C. Growth of YBCO film on MTO buffered single crystal substrate.

The formed (*h*00) oriented terraces could be beneficial for subsequent epitaxial layer growth, as the nucleation mechanism can then be supported by the ledges present at the surface [26]. Also, the buffer layers are required to act as a texture template or texture transfer layer depending on the substrate approach. This so-called texture transfer is limited by the lattice parameter and the occupation of sites in the crystal lattice [27]. So, the lattice mismatch between the buffer and the superconducting layers should be as low as possible. Table I shows the calculated lattice parameter *a* from XRD patterns (Figure 4) and is compared with lattice parameter of $YBCO_6$ (a = 3.86 Å). The lattice mismatch ε is generally defined as:

$$\varepsilon = \left|\frac{a_s - a_f}{a_s}\right| \text{ x } 100$$

With a_s and a_f the lattice parameter of the substrate and the film respectively. When this mismatch is high, the texture transfer can be inhibited leading to polycrystalline films with poor superconducting performances. To test the texture of *M*TO films and its mismatch, YBCO film was deposited with low-fluorine based CSD method. From the SEM analysis (Figure 6), it can be seen that different surface morphologies are formed. YBCO surface grown on CTO film show (00*l*) oriented and is similar as reported by Rijckaert et al.[16] as it shows small lattice mismatch of 1.05%. STO film has also small lattice mismatch with YBCO but show the presence of a/b oriented YBCO on SEM image, indicating the thermal process of low-fluorine based YBCO is not optimized yet as the a/b-oriented YBCO grains are preferred over c-oriented YBCO grains, leading to a needle shaped structure on top of the YBCO layer (Figure S4). This is due to the faster growth of a/b-grains along the (100)/(010) plane [16]. BTO film has large mismatch with YBCO and results in the formation of random YBCO as observed on SEM image (Figure 6). It is also confirmed via XRD patterns (Figure 7), showing (00*l*) YBCO reflections (2θ = 30.6° (004), 38.5° (005), and 46.6° (006)) for YBCO grown on CTO and STO films. However, STO films shows the presence of a/b oriented YBCO (2θ = 47.4°). The XRD patterns of YBCO grown on BTO films show weak YBCO reflections but two reflections at 2θ = 41.7° and 45.5° and are related to $Ba_xCu_yO_z$ and $BaTiO_3$. It indicates that YBCO grown is probably not optimized due to the outgrowth of the Ba-containing CuO_x phase at the interface of $BaTiO_3$ film. So, the low YBCO quality of STO and BTO films can be assigned by the higher roughness of the buffer layers. For these reasons, the deposition of CTO films are believed to be suitable for the YBCO growth in terms of crystallinity and morphology. The next step is to analyze the relationship between the superconducting properties of YBCO grown on *M*TO films and the texture of *M*TO films. It can simplify the cumbersome transfer of these results from *M*TO films on single crystal substrate to industrial metallic tape for the commercial market.

IV. CONCLUSION

In this work, (h00) oriented *M*TO thin films were prepared and optimized by a chemical solution deposition method based on metal trifluoroacetate and modified $TiO(acac)_2$ in methanol. These *M*TO films show different film morphologies by SEM, leading to different YBCO morphologies (as confirmed via SEM and XRD). It suggests that (1) the roughness and crystallinity of *M*TO films and (2) the lattice mismatch between *M*TO and YBCO are crucial for the film formation mechanism. From our results it can be clearly seen that the choice of the buffer film has a marked influence on the resulting YBCO texture properties.

ACKNOWLEDGMENT

The authors would like to thank Glen Verbeken (Ghent University) for TGA measurements and Laura Van Bosselle (Ghent University) for offset XRD measurements and helpful discussions.

REFERENCES

[1] D. Larbalestier, A. Gurevich, D. M. Feldmann, and A. Polyanskii, "High-T_c superconducting materials for electric power applications," Nature, vol. 414, no. 6861, pp. 368-377, 2001, doi: 10.1142/9789814317665_0046
[2] J. L. MacManus-Driscoll and S. C. Wimbush, "Processing and application of high-temperature superconducting coated conductors," Nat. Rev. Mater., pp. 1-18, 2021, doi: 10.1038/s41578-021-00290-3.
[3] J. Díez-Sierra *et al.*, "All-chemical $YBa_2Cu_3O_{7-\delta}$ coated conductors with preformed $BaHfO_3$ and $BaZrO_3$ nanocrystals on Ni5W technical substrate at the industrial scale," Supercond Sci Technol, vol. 34, no. 11, p. 114001, 2021, doi: 10.1088/1361-6668/ac2495.

© 2023 IEEE. Personal use is permitted, but republication/redistribution requires IEEE permission. See https://www.ieee.org/publications/rights/index.html for more information.
Authorized licensed use limited to: University of Gent. Downloaded on January 24,2023 at 08:34:40 UTC from IEEE Xplore. Restrictions apply.

[4] X. Obradors *et al.*, "Progress towards All-chemical Superconducting $YBa_2Cu_3O_7$-Coated Conductors," Supercond. Sci. Technol., vol. 19, no. 3, pp. S13-S26, 2006, doi: 10.1088/0953-2048/19/3/003.

[5] N. Van de Velde, T. Bruggeman, L. Stove, G. Pollefeyt, O. Brunkahl, and I. Van Driessche, "Influence of Morphology and Texture of CeO_2 on $YBa_2Cu_3O_7$ (YBCO) Growth and $BaCeO_3$ Formation in Solution-Derived Synthesis," Eur. J. Inorg. Chem., vol. 2012, no. 8, pp. 1186-1194, 2012, doi: 10.1002/ejic.201100951.

[6] L. Piperno *et al.*, "Interaction between untreated $SrTiO_3$ substrates and solution-derived $YBa_2Cu_3O_{7-\delta}$ films," Appl. Surf. Sci., vol. 528, p. 146402, 2020, doi: 10.1016/j.apsusc.2020.146402.

[7] G. Pollefeyt, S. Clerick, P. Vermeir, P. Lommens, K. De Buysser, and I. Van Driessche, "Influence of Aqueous Precursor Chemistry on the Growth Process of Epitaxial $SrTiO_3$ Buffer Layers," Inorg. Chem., vol. 53, no. 10, pp. 4913-4921, 2014, doi: 10.1021/ic403067h.

[8] H. Zhang *et al.*, "Epitaxial growth of $CaTiO_3$ buffer layer for fabrication of c-axis oriented YBCO film by sol-gel method," J. Sol-Gel Sci. Technol., vol. 82, no. 1, pp. 45-50, 2017, doi: 10.1007/s10971-016-4282-y.

[9] R. W. Schwartz *et al.*, "Control of Microstructure and Orientation in Solution-Deposited $BaTiO_3$ and $SrTiO_3$ Thin Films," J. A. Ceram. Soc., vol. 82, no. 9, pp. 2359-2367, 1999, doi: 10.1111/j.1151-2916.1999.tb02091.x.

[10] U. Hasenkox, S. Hoffmann, and R. Waser, "Influence of precursor chemistry on the formation of $MTiO_3$ (M= Ba, Sr) ceramic thin films," J. Sol-Gel Sci. Technol., vol. 12, no. 2, pp. 67-79, 1998, doi: 10.1023/A:1026480027046.

[11] H. Rijckaert *et al.*, "Microwave-Assisted $YBa_2Cu_3O_7$ Precursors: A Fast and Reliable Method towards Chemical Precursors for Superconducting Films," J. Am. Ceram. Soc, vol. 100, no. 6, pp. 2407–2418, 2017, doi: 10.1111/jace.14757.

[12] T. Araki and I. Hirabayashi, "Review of a chemical approach to $YBa_2Cu_3O_{7-x}$-coated superconductors—metalorganic deposition using trifluoroacetates," Supercond. Sci. Technol., vol. 16, no. 11, pp. R71-R94, 2003, doi: 10.1088/0953-2048/16/11/R01.

[13] M. P. Siegal, P. G. Clem, J. T. Dawley, J. Richardson, D. L. Overmyer, and T. G. Holesinger, "Optimizing $SrTiO_3$ films on textured Ni substrates using chemical solution deposition," J. Mater. Res., vol. 20, no. 4, pp. 910-921, 2005, doi: 10.1557/JMR.2005.0137.

[14] J. Kunert *et al.*, "Advanced titania buffer layer architectures prepared by chemical solution deposition," Supercond. Sci.Technol., vol. 24, no. 8, p. 085018, 2011, doi: 10.1088/0953-2048/24/8/085018.

[15] M. Bäcker, M. Falter, O. Brunkahl, and B. Holzapfel, "Superconducting Films," in *Chemical solution deposition of functional oxide thin films*, T. Schneller, R. Waser, M. Kosec, and D. Payne Eds.: Springer, 2013, ch. 27, pp. 673-705.

[16] H. Rijckaert, J. Hänisch, G. Pollefeyt, M. Bäcker, and I. Van Driessche, "Influence of Ba^{2+} consumption and intermediate dwelling during processing of $YBa_2Cu_3O_7$ nanocomposite films," J. Am. Ceram. Soc., vol. 102, no. 7, pp. 3870-3878, 2019, doi: 10.1111/jace.16228.

[17] J. Huijbregtse, J. Rector, and B. Dam, "Effect of the Two (100) $SrTiO_3$ Substrate Terminations on the Nucleation and Growth of $YBa_2Cu_3O_{7-\delta}$ Thin Films," Physica C, vol. 351, no. 3, pp. 183-199, 2001, doi: 10.1016/S0921-4534(00)01616-6.

[18] P. Vermeir, F. Deruyck, J. Feys, P. Lommens, J. Schaubroeck, and I. Van Driessche, "Comments on the wetting behavior of non-porous substrates for ceramic coated-conductor applications," (in English), J Sol-Gel Sci Technol, vol. 62, no. 3, pp. 378-388, 2012/06/01 2012, doi: 10.1007/s10971-012-2737-3.

[19] N. Roma *et al.*, "Acid anhydrides: a simple route to highly pure organometallic solutions for superconducting films," Supercond. Sci. Technol., Article vol. 19, no. 6, pp. 521-527, Jun 2006, doi: 10.1088/0953-2048/19/6/019.

[20] A. Gupta, R. Jagannathan, E. I. Cooper, E. Giess, J. Landman, and B. Hussey, "Superconducting oxide films with high transition temperature prepared from metal trifluoroacetate precursors," Appl. Phys. Lett., vol. 52, no. 24, pp. 2077-2079, 1988, doi: 10.1063/1.99752.

[21] R. Schwartz, J. Voigt, B. Tuttle, D. Payne, T. Reichert, and R. DaSalla, "Comments on the effects of solution precursor characteristics and thermal processing conditions on the crystallization behavior of sol-gel derived lead zirconate titanate thin films," J. Mater. Res., vol. 12, no. 2, pp. 444-456, 1997, doi: 10.1557/JMR.1997.0066.

[22] A. Leaustic, F. Babonneau, and J. Livage, "Structural investigation of the hydrolysis-condensation process of titanium alkoxides $Ti(OR)_4$ (OR= OPr-iso, OEt) modified by acetylacetone. 1. Study of the alkoxide modification," Chem. Mater., vol. 1, no. 2, pp. 240-247, 1989, doi: 10.1021/cm00002a015.

[23] X. Obradors *et al.*, "Chemical solution deposition: a path towards low cost coated conductors," Supercond. Sci. Technol. , vol. 17, no. 8, p. 1055, 2004, doi: 10.1088/0953-2048/17/8/020.

[24] W.-N. Shen, B. Dunn, C. Moore, M. Goorsky, T. Radetic, and R. Gronsky, "Synthesis of nanoporous bismuth films by liquid-phase deposition," J. Mater. Chem., vol. 10, no. 3, pp. 657-662, 2000, doi: 10.1039/A907581J.

[25] P. Clem *et al.*, "Epitaxial Solution Deposition of $YBa_2Cu_3O_{7-\delta}$-Coated Conductors," Int. J. Appl. Ceram, vol. 2, no. 1, pp. 24-32, 2005, doi: 10.1111/j.1744-7402.2005.02005.x.

[26] Y. Xu *et al.*, "Preparation of YBCO films on CeO_2-buffered (001) YSZ substrates by a non-fluorine MOD method," J. Am. Ceram. Soc., vol. 87, no. 9, pp. 1669-1676, 2004, doi: 10.1111/j.1551-2916.2004.01669.x.

[27] J. M. Phillips, "Substrate selection for high-temperature superconducting thin films," J. Appl. Phys., vol. 79, no. 4, pp. 1829-1848, 1996, doi: 10.1063/1.362675.

© 2023 IEEE. Personal use is permitted, but republication/redistribution requires IEEE permission. See https://www.ieee.org/publications/rights/index.html for more information.

Authorized licensed use limited to: University of Gent. Downloaded on January 24,2023 at 08:34:40 UTC from IEEE Xplore. Restrictions apply.